Sensors and Materials, Vol. 35, No. 12 (2023) 4167–4176
MYU Tokyo

S & M 3474

Sensitive and Selective Electrochemical Sensor for Antimony Using Boron-doped Diamond Nanoparticles

Prastika Krisma Jiwanti,[1*] Moh. Agus Rismafullah,[2] Aning Purwaningsih,[2] Md Shalauddin,[3] Shamima Akhter,[4] Wan Jeffrey Basirun,[3,4] and Intan Nurul Rizki[1]

[1]Nanotechnology Engineering, Faculty of Advanced Technology and Multidiscipline, Universitas Airlangga, Surabaya 60115, Indonesia
[2]Department of Chemistry, Faculty of Science and Technology, Universitas Airlangga, Surabaya 60115, Indonesia
[3]Nanotechnology and Catalysis Research Center (NANOCAT), University Malaya, Kuala Lumpur 50603, Malaysia
[4]Department of Chemistry, Faculty of Science, University Malaya, Kuala Lumpur 50603, Malaysia.

(Received July 24, 2023; accepted August 23, 2023)

Keywords: antimony, boron-doped diamond, screen-printed electrode, clean water

In this study, boron-doped diamond nanoparticles modified on the surface of a screen-printed electrode (SPE) were prepared for the sensitive and selective determination of Sb^{3+} using square wave voltammetry. The effect of electrochemical parameters such as the type of supporting electrolyte, pH, signal per background, and scan rate on the sensitivity of the sensor for the detection of Sb^{3+} was investigated. Under optimized conditions with an amplitude of 0.05 V, a frequency of 50 Hz, and an E-step of 0.05 V, the square wave voltammogram between −1.0 and 1.0 V gave a limit of detection of 2.41×10^{-8} M for an Sb^{3+} concentration range from 0.19 to 0.59 μM. The method was used to determine Sb^{3+} ions in river water with satisfactory results. The modified electrode displayed benefits such as high sensitivity and selectivity, long-term stability, easy preparation, and wide linear range.

1. Introduction

Some toxic metal ions are widely distributed in water and food resources owing to human activities. One such metal ion is antimony (Sb), which is toxic and causes serious problems to human health, such as dizziness, headache, and depression, at low doses of around 2.15 μg/L, and it damages the kidneys and heart at higher doses of around 9 μg/L.(1) Sb and its compounds are toxic, and Sb(III) possesses a high affinity towards red blood cells and the sulfhydryl groups that are the constituents of those cells.(2) Sb is utilized in the production of ceramic materials, glass, polymerization catalysts, pharmaceuticals, pigments, textiles, paper, and especially polyethylene terephthalate, which is widely used in the packaging of alcoholic and nonalcoholic beverages.(3) Thus, the rapid and sensitive detection of heavy metals at trace levels in fresh water sources is becoming very important as heavy metal ions have serious toxicological effects on living organisms.(4)

*Corresponding author: e-mail: prastika.krisma@ftmm.unair.ac.id
https://doi.org/10.18494/SAM4599

ISSN 0914-4935
https://myukk.org/

Several different techniques are utilized for the detection of Sb^{3+}, such as spectroscopy, chromatography, and electrochemistry.(5) However, the spectroscopic and chromatographic techniques are time-consuming and cumbersome, and are also unsuited for the *in situ* measurements of metal ions owing to the complexity of the instruments. In contrast, electrochemical techniques are becoming important as they are cost-effective, portable, and easy to operate.(6,7) Square wave voltammetry (SWV) is considered one of the sensitive electroanalytical techniques for the determination of trace quantities of heavy metal ions.(8)

Meanwhile, the screen-printed electrode (SPE) has gained popularity as it is an alternative to traditional electrodes for the development of a rapid *in situ* analytical method.(9) Nanomaterials are an attractive choice for the development of SPE, as they enhance the sensitivity of electrodes for a particular analyte species.(10) The modification of the SPE with nanomaterials such as boron-doped diamond nanoparticles (BDDNPs) improves the limit of detection (LOD).(11) BDDNPs can be used as modifiers in SPE, as they possess several advantages such as high sensitivity due to the wide potential window and low background current.(12) BDDNPs have several characteristics that are appropriate as coatings of working electrodes (WEs), such as an inert surface with low adsorption, long service life with high stability and performance, and corrosion resistance even in strong acidic media. In this study, BDDNPs are modified on SPE (SPDE) for the detection of Sb^{3+} ions in river water samples. The SPDE modification results in a larger surface area for detection; thus, more Sb^{3+} ions can be detected on the electrode surface with highly sensitive measurements.

2. Materials and Methods

2.1 Chemicals

All chemicals used were of analytical reagent grade. Glacial acetic acid (CH_3COOH, ≥99.7%) and sodium acetate (CH_3COONa, ≥99.0%) were obtained from Sigma Aldrich (USA). Standard solutions of iron [$Fe(NO_3)_3$] in HNO_3 (1000 mg/L), lead [$Pb(NO_3)_2$] in HNO_3 (1000 mg/L), cobalt [$Co(NO_3)_2$] in HNO_3 (1000 mg/L), and cadmium [$Cd(NO_3)_2$] in HNO_3 (1000 mg/L) were obtained from Merck (Germany), whereas BDDNPs with sizes between 0 and 250 nm were purchased from Hunan Boromond EPT (China). SPE was purchased from TailKuKe (China). All chemicals were used without further purification.

2.2 Instrumentations

SWV experiments were carried out using an automated handheld power-driven PalmSens electrochemical analyzer (PalmSens BV, The Netherlands). The SPE for this study comes with a carbon WE strip, a carbon auxiliary electrode strip, and a silver reference electrode strip embossed on a plastic substrate. The functional groups of nanocomposites were identified by Fourier transform infrared spectroscopy (FTIR, IR Tracer-100, Shimadzu, Japan) and were recorded in the range of 500–4000 cm^{-1}. A UV–visible scanning spectrophotometer (UV–Vis, Shimadzu UV-1800, Japan) and X-ray diffraction (XRD, PANalytical B.V, Netherlands) were

used to investigate the constituents of the nanocomposite. The surface morphology of the BDDNP-modified SPE was studied using a field emission scanning electron microscope (FESEM, JEOL JSM-7600F) attached with an energy-dispersive X-ray (EDX) spectrometer.

2.3 Preparation of modified electrode and electrochemical analysis

The BDDNP ink was prepared by mixing 10 mg of BDDNPs in 0.5 mL of 30% ethanol using an ultrasonicator until the BDDNPs were completely dispersed. To prepare SPDE, the modification was carried out by drop-casting the BDDNP ink suspension (20 μL) onto the surface of the WE part of the SPE and dried at 60 °C for 90 min in an oven. The drying of the modified SPE in the oven evaporates the solvent and prevents the BDDNPs from leaching out during the experiments.

All electrochemical measurements were carried out by pipetting 1.33 μL of 60 μM Sb^{3+} in 60 μL of 0.1 M acetate buffer solution and drop casting onto the SPE. Cyclic voltammetry (CV) and SWV were performed with a Sensit smart Palmsens potentiostat. The mixed solution was allowed to equilibrate for 5 s before scanning from −1 to 1 V at an amplitude of 0.05 A, a frequency of 50 Hz, and an E-step of 0.05 V.

3. Results and Discussion

3.1 Characterization of modified electrode

Figure 1(a) shows the FESEM image of the surface of the SPDE. The FESEM image provides useful information about the surface topography of the sample on the surface of the WE. The FESEM image of the SPDE reveals a homogeneous and nonporous surface morphology. From the analysis performed using the ImageJ software, the average size of the SPDE was found to be 192.22 nm. The XRD pattern of the BDDNP material confirms that the peaks at 2θ = 43, 85 and 75°, 36° correspond to the lattice planes of (111) and (220) of diamond, respectively [Fig. 1(b)].[13] The FTIR spectrum of SPDE in Fig. 1(c) shows medium or strong bands at 2168, 1630, 1438, and 1092 cm^{-1}. The main peaks in the spectrum are related to the boron–carbon (B–C) vibration at 1438 cm^{-1}. These peaks have been identified and associated with substitutional boron in diamond.[14] On the other hand, the band at 1092 cm^{-1} is assigned to the boron–oxygen (B–O) species present on the grain boundaries. The band of the carbonyl group at 1630 cm^{-1} indicates the possible oxidation of the sp^2 bond. Figure 1(d) shows the UV–vis spectrum of the SPDE, where a prominent absorption spectrum is observed at approximately 242 nm, which corresponds to the electronic transition of the boron atom in the BDD lattice.[14]

3.2 Electrochemical characterization of antimony

3.2.1 Signal per background (S/B)

The measurement of the signal per background (S/B) on the SPE and SPDE is useful for studying the sensitivity of Sb^{3+} analysis. The S/B on the SPE and SPDE was determined by the

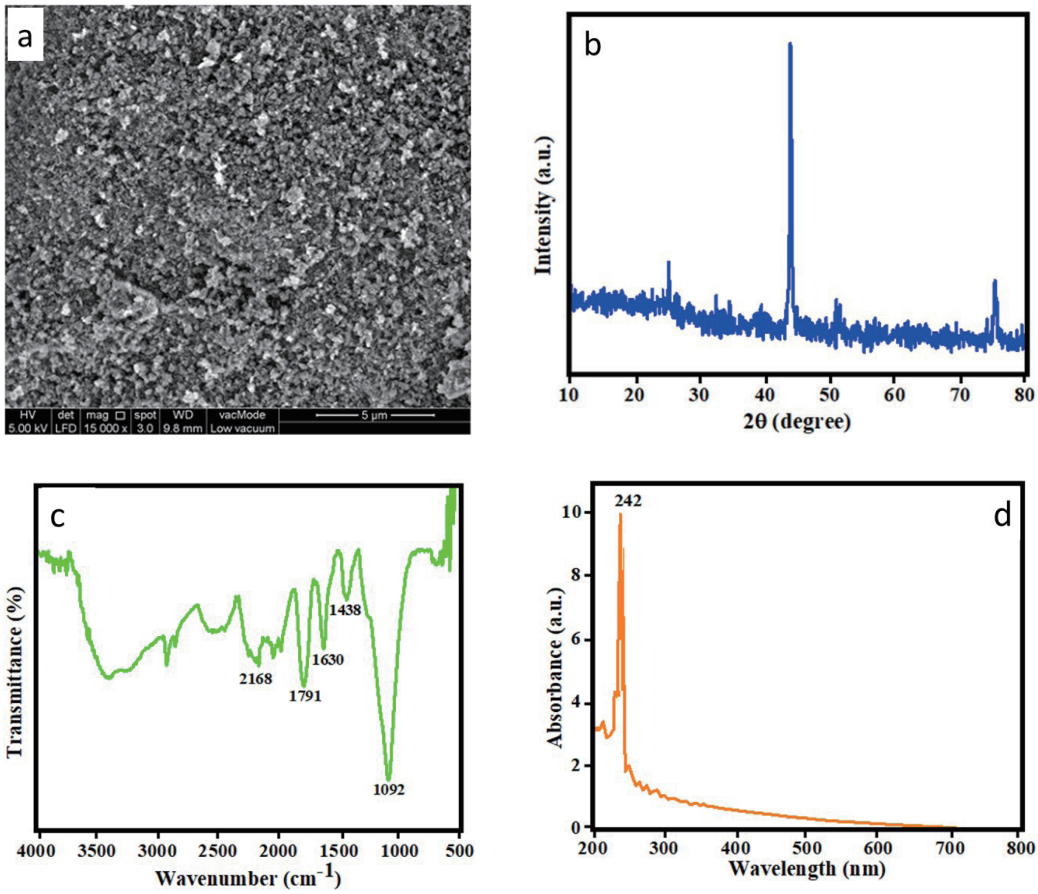

Fig. 1. (Color online) (a) FESEM image of surface of SPDE, (b) XRD pattern of SPDE, (c) FTIR spectrum of SPDE, and (d) UV–vis spectrum of SPDE.

SWV method. The quotients between the peak signal current and the background in the SPE and SPDE are 4.648 and 12.052, respectively (Fig. 2). It is confirmed that the SPDE provides a higher S/B signal ratio than does the SPE, which provides better sensitivity, at the same concentration, where the resulting sample current signal was greater than that with SPE. The use of nanomaterials as modifiers results in a larger surface area of SPDE, more active sites, and higher adsorption.[15]

3.2.2 Effect of scan rate variation

The scan rate variation of Sb^{3+} on the SPE and SPDE was determined by the CV method. Scan rate measurements were carried out with scan rate variations of 40, 50, 60, 70, 80, 90, and 100 mV/s. The current peak shifts to a more positive linear potential value with the increase in the scan rate, indicating quasi-irreversibility in the electro-oxidation process.[16]

Figure 3 shows that the peak current increases with the scan rate. The peak current was higher in SPDE than in SPE, indicating that the transfer of electrons occurred faster on the

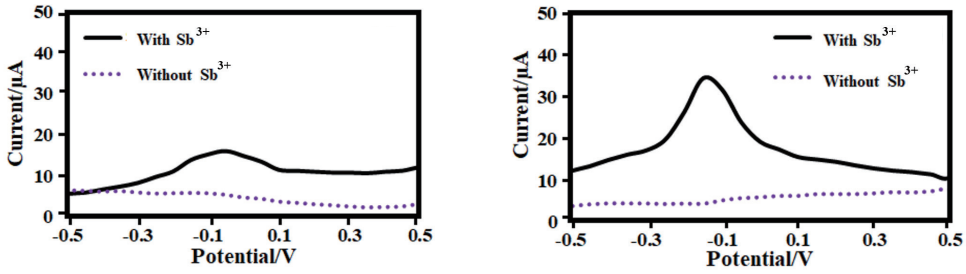

(a) (b)

Fig. 2. (Color online) SWV voltammogram of 0.39 µM Sb^{3+} in 0.1 M acetate buffer when using (a) SPE and (b) SPDE in the determination of S/B ratio.

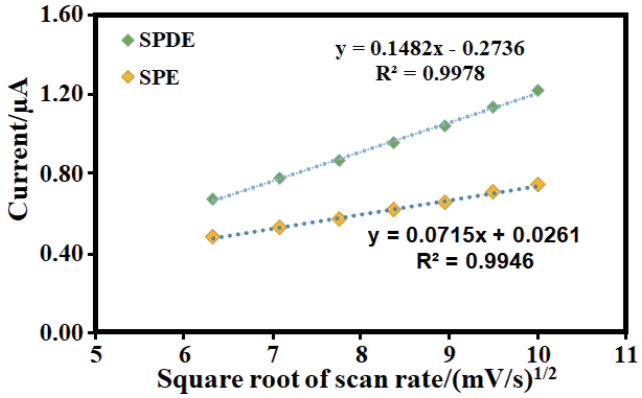

Fig. 3. (Color online) Calibration plot of peak current vs root scan rate in 0.39 µM Sb^{3+} in 0.1 M acetate buffer with pH 4.5 over a scan rate variation range of 40–100 mV/s.

surface area of SPDE. A larger scan rate promotes a faster ion diffusion towards the electrode surface, which causes a greater current response.[17] Figure 3 also shows a linear plot between the anodic and cathodic peak currents as a function of the square root of the scan rate, for the redox reaction in 0.39 µM Sb^{3+} in 0.1 M acetate buffer at pH 4.5, with the curves of the linear regression equations of I_{pa} (A) = $0.0715v^{0.5}$ − (mV/s)$^{0.5}$ − 0.0261 (R^2 = 0.9949) and I_{pa} (A) = $0.1482v^{0.5}$– (mV/s)$^{0.5}$–0.2736 (R^2 = 0.9978), for the SPE and SPDE, respectively. This confirms that the electron transfer at the electrode is diffusion controlled.

3.2.3 Effect of pH

The electrochemical performance of the fabricated electrodes is significantly affected by the pH of the solution medium. The pH values of the acetate buffer are 3, 3.5, 4, 4.5, 5, and 5.5. The current increases with the pH of the solution but decreases after reaching the pH with the

maximum current. The acetate buffer was selected as the solution in this study as the acetate buffer solution contains a CH_3COO^- group that forms a complex compound with the antimony ions ($Sb\text{-}CH_3COO^{2+}$), which stabilizes the Sb^{3+} ions and supports the anodic stripping.[6] The formation of the complex compound $Sb\text{-}CH_3COO^{2+}$ in the proposed system is as follows.

$$Sb(OH)_3 + 3H^+ + CH_3COO^- \rightarrow 3H_2O + Sb(CH_3COO)^{2+} \quad (1)$$

$$Sb(OH)_3 + 3H^+ + 2CH_3COO^- \rightarrow 3H_2O + Sb(CH_3COO)_2^+ \quad (2)$$

Figure 4 shows plot of peak potential and peak current vs pH. It was confirmed that the maximum current peak was obtained at a pH of 4.5, which is attributed to the greater adsorption of the Sb^{3+} reduction product on the electrode surface. The difference in pH also affects the peak potential; thus, the peak potential at each pH differs from one another. As a result, at a fairly low pH, a large amount of added H^+ will promote the equilibrium reaction to shift towards a negative potential; therefore, the oxidation process requires a higher potential.[18] Finally, it can be concluded that the lower the pH, the more the response of the oxidation current shifts towards a positive potential, and with higher pH, the response of the oxidation current shifts towards a negative potential.[19]

3.3 Sensitivity and limit of detection

Sb^{3+} was quantitatively analyzed on SPDE by the SWV method. The Sb^{3+} peak current is linear in the concentration range from 0.19 to 0.59 μM, including blank measurements. Figure 5 shows voltammograms and a linear correlation between the Sb^{3+} concentration and the current response with the equation $y = 29.18x + 19.1$ (R^2=0.9974) (inset). By employing the $3S_b/m$, S_b = standard deviation of the blank sample and m = slope of the calibration graph,[20,21] the LOD becomes 2.41×10^{-8} M. The sensitivity of the SPDE is expressed by the gradient (y/x) in the regression equation and is 29.18 (μA/μM). The analytical performance of the Sb^{3+} detection using various modified WEs was reported previously. It can be concluded from Table 1 that the LOD of Sb^{3+} on the SPDE is comparable to those shown in previous reports. In addition, the proposed work in SPDE has the advantages of simplicity, portability, and environmental friendliness compared with the use of Hg with a comparable LOD.

3.4 Interference study

The selectivity of the sensor electrode is defined by its ability to accurately detect the target analyte in the presence of other interferent components that may be present in the sample matrix. The selectivity of the proposed sensor for the detection of Sb^{3+} was determined by studying the effects of interferent metal ions (Cd^{2+}, Fe^{3+}, Co^{2+}, and Pb^{2+}) that are present together with Sb^{3+} in natural water by the SWV technique under optimum conditions. The interferent metals were chosen on the basis of a previous article in which it was stated that Cd^{2+}, Fe^{3+}, Co^{2+}, and Pb^{2+} metals have a great impact on Sb^{3+} signal peaks.[22] Sb^{3+} was first measured in the absence of

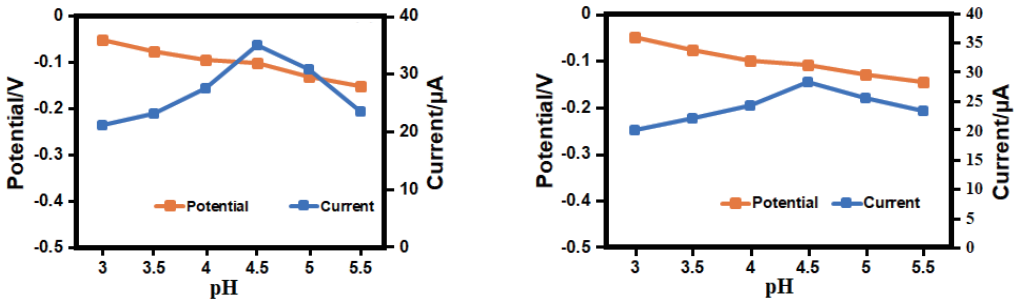

Fig. 4. (Color online) Plot of peak potential and peak current vs pH of Sb^{3+} 0.39 μM in 0.1 M acetate buffer at pH 3–5.5 using (a) SPE and (b) SPDE.

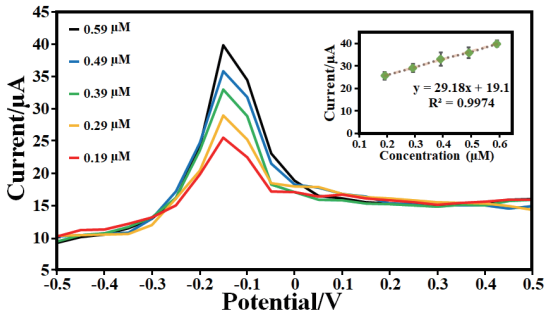

Fig. 5. (Color online) SWV voltammogram of 0.39 μM Sb^{3+} in 0.1 M acetate buffer of pH 4.5 using SPDE over a concentration variation range of 0.19–0.59 μM. (Inset) Linear correlation between Sb^{3+} concentration vs current response using SPDE in the variation range of 0.19–0.59 μM.

Table 1
LOD values of Sb^{3+} measurements using various electrodes.

Method	Working Electrode	LOD	Ref.
DPSV	AuNPs/CPE	6.67×10^{-8} M	23
DPASV	SPE/Hg	1.27×10^{-8} M	24
SWASV	GC/rGO	4.90×10^{-8} M	22
SWV	SPDE	2.41×10^{-8} M	This work

interferent metal ions, then, in the presence of the interferent metal ions at a concentration ratio of 1:1. The voltammogram of the selectivity between Sb and the interferent metal ions is shown in Fig. 6.

3.5 Analytical application of developed electrode

The application of the modified electrode in real samples was tested by determining the concentration of Sb^{3+} in river water. In general, the Sb^{3+} concentration in river water is around 1.1 μg/L. The level of precision was evaluated by spiking the sample with a typical Sb^{3+} solution. The samples spiked with Sb^{3+} show excellent recovery (Table 2). This confirms that the process

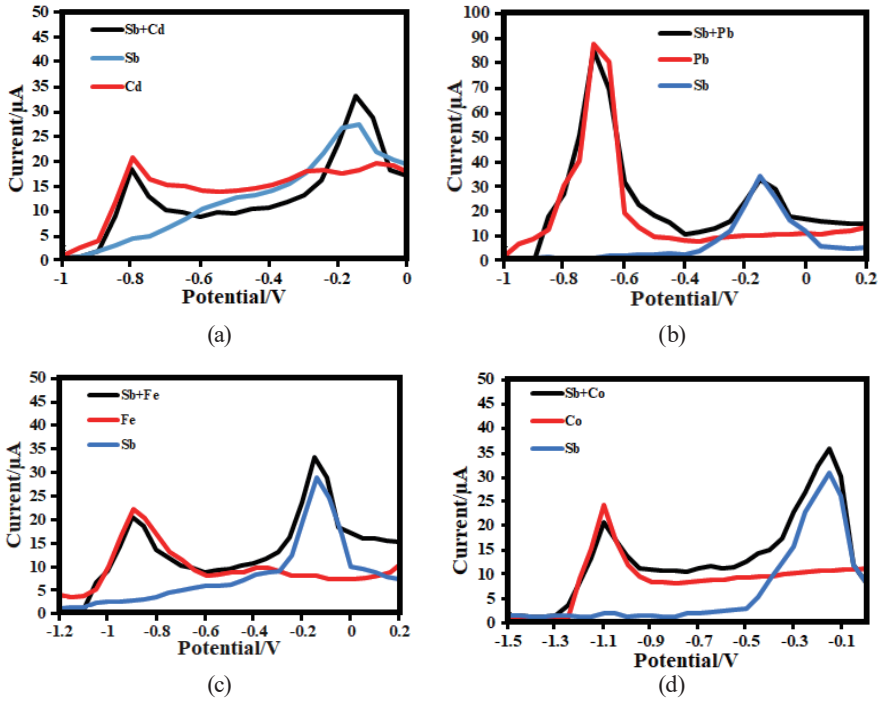

Fig. 6. (Color online) Selectivity of Sb^{3+} with interferents (a) Cd^{2+}, (b) Co^{2+}, (c) Fe^{3+}, and (d) Pb^{2+} in 0.1 M acetate buffer pH 4.5 using SPDE.

Table 2
Analysis of Sb^{3+} in river water samples.

Sample	Electrode	Sb added (μM)	Sb found (μM)	% Recovery	% RSD
River water	SPE	0.39	0.40	102	0.31
	SPDE	0.39	0.42	107	0.74

is selective and appropriate for the determination of Sb^{3+} in real samples. SPE yielded more accurate and stable results, because the surface area of SPDE modified with BDDNP was not more stable than that of the SPE without modification. These results indicate that the SPE and SPDE can be utilized for the detection of Sb^{3+} in real samples by the SWV method with high accuracy. In addition, the relative standard deviation (RSD) of the measurements is lower than 5%. This indicates that the proposed method and modification can meet the requirements for a high-performance Sb^{3+} sensor for real samples.

4. Conclusions

An innovative BDDNP-modified SPE was developed for the stripping analysis of Sb^{3+}. This electrode was derived by merging the distinctive features of BDDNPs. The effectiveness of the electrode was demonstrated by its ability to detect Sb^{3+} ions in river water samples in the presence of other Cd^{2+}, Fe^{3+}, Co^{2+}, and Pb^{2+} ions. The modified electrode sensor possesses high sensitivity as well as high selectivity for the detection of Sb^{3+} ions.

Acknowledgments

This research was funded by Direktorat Riset, Teknologi, dan Pengabdian Kepada Masyarakat, Kementerian Pendidikan, Kebudayaan, Riset, dan Teknologi Republik Indonesia 2023 with contract number 1339/UN3.LPPM/PT.01.03/2023.

References

1. T. H. A. Hasanin, T. Yamamoto, Y. Okamoto, S. Ishizaka, and T. Fujiwara: Anal. Sci. **32** (2016) 245. https://doi.org/10.2116/analsci.32.245
2 G. Wen, X. Zhang, Y. Li, Y. Luo, A. Liang, and Z. Jiang: Food Chem. **214** (2017) 25. https://doi.org/10.1016/j.foodchem.2016.07.050
3 R. S. Multani, T. Feldmann, and G. P. Demopoulos: Hydrometallurgy **164** (2016) 141. https://doi.org/10.1016/j.hydromet.2016.06.014
4 N. R. Biata, L. Nyaba, J. Ramontja, N. Mketo, and P. N. Nomngongo: Food Chem. **237** (2017) 904. https://doi.org/10.1016/j.foodchem.2017.06.058
5 D. Atakan, İ. Durukan, and S. Bektas: Anal. Lett. **49** (2016) 1066. https://doi.org/10.1080/00032719.2015.1067811
6 M. Shalauddin, S. Akhter, W. J. Basirun, V. S. Lee, Ab R. Marlinda, S. R. Ahmed, A. R. Rajabzadeh, and S. Srinivasan: Electrochim. Acta **454** (2023) 142423. https://doi.org/10.1016/j.electacta.2023.142423
7 M. Shalauddin, S. Akhter, W. J. Basirun, M. Akhtaruzzaman, M. A. Mohammed, N. M. M. A. Rahman, and N. M. Salleh: Surf. Interfaces, **34** (2022) 102385. https://doi.org/10.1016/j.surfin.2022.102385
8 F. R Simões and M. G. Xavier: Electrochemical Sensors. In Nanoscience and Its Applications (Elsevier, 2017).
9 P. K. Jiwanti, B. Wardhana, L. G. Sutanto, D. M. M. Dewi, I. Z. D. Putri, and I. N. I. Savitri: Molecules **27** (2022) 7578. https://doi.org/10.3390/molecules27217578
10 S. Akhter, Md. Shalauddin, W. J. Basirun, V. S. Lee, S. R. Ahmed, A. R. Rajabzadeh, and S. Srinivasan: Sens. Actuators, B **373** (2022) 132743. https://doi.org/10.1016/j.snb.2022.132743
11 T. Matsunaga, T. Kondo, T. Osasa, A. Kotsugai, I. Shitanda, Y. Hoshi, M. Itagaki, T. Aikawa, T. Tojo, and M. Yuasa: Carbon **159** (2020) 247. https://doi.org/10.1016/j.carbon.2019.12.051
12 T. Kondo, M. Kikuchi, H. Masuda, F. Katsumata, T. Aikawa, and M. Yuasa: J. Electrochem Soc. **165** (2018) F3072. https://doi.org/10.1149/2.0111806jes
13 Y. V. Pleskov, M. D. Krotova, V. V. Elkin, and E. A. Ekimov: Electrochim Acta. **201** (2016) 268. https://doi.org/10.1016/j.electacta.2015.09.075
14 M. Ensch, V. Y. Maldonado, G. M. Swain, R. Rechenberg, M. F. Becker, T. Schuelke, and C. A. Rusinek: Anal. Chem, **90** (2018) 1951. https://doi.org/10.1021/acs.analchem.7b04045
15 T. Ochiai, S. Tago, M. Hayashi, K. Hirota, T. Kondo, K. Satomura, and A. Fujishima: Electrochem Commun. **68** (2016) 49. https://doi.org/10.1016/j.elecom.2016.04.011
16 Y. Wang, B. Huang, W. Dai, J. Ye, and B. Xu: J. Electroanal. Chem. **776** (2016) 93. https://doi.org/10.1016/j.jelechem.2016.06.031
17 V. C. G. dos Santos, M. T Grassi, and G. Abate: Anal. Lett. **48** (2015) 2921. https://doi.org/10.1080/00032719.2015.1052971
18 T. E. Chiwunze, V. N. Palakollu, A. A. S. Gill, F. Kayamba, N. B. Thapliyal, and R. Karpoormath: Mater. Sci. Eng. C **97** (2019) 285. https://doi.org/10.1016/j.msec.2018.12.018
19 Y. Zeng, D. Chen, T. Chen, M. Cai, Q. Zhang, Z. Xie, R. Li, Z. Xiao, G. Liu, and W. Lv: Chemosphere **227** (2019) 198. https://doi.org/10.1016/j.chemosphere.2019.04.039
20 M. Shalauddin, S. Akhter, W. J. Basirun, N. S. Anuar, O. Akbarzadeh, M. A. Mohammed, and M. R. Johan: Measurement **194** (2022) 110961. https://doi.org/10.1016/j.measurement.2022.110961
21 M. Shalauddin, S. Akhter, W. J. Basirun, V. S. Lee, and M. R. Johan: Environ. Nanotechnol. Monit. Manag. **18** (2022) 100691. https://doi.org/10.1016/j.enmm.2022.100691
22 F. Liendo, A. P. de la Vega, M. Jesus Aguirre, F. Godoy, A. A. Martí, E. Flores, J. Pizarro, and R. Segura: Food Chem. **367** (2022) 130676. https://doi.org/10.1016/j.foodchem.2021.130676
23 R. Liu, Y. J. Tan, T. Zhong, C. Lei: Anal. Lett. **51** (2018) 2351. https://doi.org/10.1080/00032719.2018.1424174
24 O. Domínguez-Renedo, M. J. G. González, and M. J. Arcos-Martínez: Sensors **9** (2009) 219. https://doi.org/10.3390/s90100219

About the Authors

Prastika Krisma Jiwanti received her B.Sc. degree from Universitas Indonesia, Indonesia, in 2010 and her M.Sc. and Ph.D. degrees from Keio University, Japan, in 2016 and 2019, respectively. From 2019 to 2022, she was an assistant professor at Universitas Airlangga. Her research interests are in electrochemistry, sensors, biosensors, and carbon materials. (prastika.krisma@ftmm.unair.ac.id)

Moh. Agus Rismafullah received his B.Sc. degree from Universitas Airlangga, Indonesia, in 2023. From 2022 to 2023, he was a researcher at Universitas Airlangga, Indonesia. His research interests are in electrochemistry, sensors, biosensors, carbon materials, and boron-doped diamond. (moh.agus.rismafullah-2019@fst.unair.ac.id)

Aning Purwaningsih received her B.Sc. and M.Sc. degrees from Universitas Airlangga, Indonesia, in 1990 and 2003, respectively. Since 2014, she has been an assistant professor at Universitas Airlangga. Her research interests are in food analysis chemistry and applied analytical chemistry. (aning-p@fst.unair.ac.id)

Md Shalauddin received his B.Sc and M.Sc. degrees in pharmacy from Primeasia University Dhaka, Bangladesh, and Ph.D. degree from NANOCAT, University of Malaya. His research interests are in the preparation of nanocomposites for energy storage and electrochemical sensors, biosensors, and piezoelectric sensors. He is now a postdoctoral research fellow in NANOCAT, University of Malaya. (pharmashalauddin@um.edu.my)

Shamima Akhter is a postdoctoral research fellow in biomedical engineering at the University of Malaya. She received her B.Sc. and M.Sc. degrees in pharmacy from Primeasia University, Bangladesh, and Ph.D. degree from the Department of Chemistry, University of Malaya. Her research interests are in electrochemistry, synthesis of nanomaterials, electrochemical sensors, and biosensors. (shamimaakhter@yahoo.com)

Wan Jefrey Basirun is a professor in the Department of Chemistry, University of Malaya. He received his Ph.D. degree from the University of Southampton, United Kingdom in 1997. His research interests are in electrochemistry, material science, and nanotechnology. (jeff@um.edu.my)